Hindawi Publishing Corporation
Journal of Sensors
Volume 2012, Article ID 617386, 6 pages
doi:10.1155/2012/617386

Research Article

Rapid and Reliable Calibration of Laser Beam Deflection System for Microcantilever-Based Sensor Setups

Rohit Mishra,[1] Wilfried Grange,[2] and Martin Hegner[1]

[1] *Centre for Research on Adaptive Nanostructures and Nanodevices and School of Physics, Trinity College Dublin, Dublin 2, Ireland*
[2] *Institut Jacques Monod, CNRS, Université Paris Diderot, 75205 Paris Cedex 13, France*

Correspondence should be addressed to Rohit Mishra, mishrar@tcd.ie and Martin Hegner, hegnerm@tcd.ie

Received 14 June 2011; Accepted 5 August 2011

Academic Editor: Martin Hegner

Cantilever array-based sensor devices widely utilise the laser-based optical deflection method for measuring static cantilever deflections mostly with home-built devices with individual geometries. In contrast to scanning probe microscopes, cantilever array devices have no additional positioning device like a piezo stage. As the cantilevers are used in more and more sensitive measurements, it is important to have a simple, rapid, and reliable calibration relating the deflection of the cantilever to the change in position measured by the position-sensitive detector. We present here a simple method for calibrating such systems utilising commercially available AFM cantilevers and the equipartition theorem.

1. Introduction

Cantilever-based sensor devices have extensively developed from the atomic force microscope (AFM) operating in the static mode [1–3] (surface stress based; qualitative method) and the dynamic mode [4–6] (frequency based; quantitative method) depending on the application. The most frequently used method of signal transduction where cantilevers are employed is change in surface stress being converted into mechanical signal through cantilever bending [7]. This deflection is an indication of the chemical [8], physical [9], or biophysical [10] process that occurs on the cantilever interface.

The laser beam-based deflection system [11] has been used most widely to measure the cantilever bending in the static mode because of the ease of use, robustness of the read-out technique, and availability of high-sensitivity position-sensitive detectors (PSDs) which allow subangstrom resolution [12, 13]. Subsequently, several studies have been made to determine the limitations of this technique along with its resolution and sensitivity [14–17]. One also comes across various techniques for determining the relation between the cantilever bending and the change in spot position observed by the PSD [18–21]. The simple geometric calculation of this factor safely presumes that the bending of the cantilever is very small such that it can be assumed to be half that of the deflection angle of the laser beam [20]. Most other methods are tedious and require specialised methods [18] for determining this factor and may additionally require precise measurement of the angles [22] (azimuthal and incidence), distance between the cantilever surface and the PSD, and so forth, which gets more complicated for beam directing methods with complex geometries using mirrors. We present here a simple plug and measure system for determining this deflection factor (G) using commercially available AFM cantilevers and applying the equipartition theorem for small cantilever deflections.

The displacement of the laser spot on the PSD (Δd) can be related to the cantilever bending (Δx) (Figure 1) using geometrical methods as [20]

$$\Delta x = \frac{\Delta d L}{4s}, \tag{1}$$

where s is the distance from cantilever to the PSD, and L is the length of the cantilever. Hence, the value of Δx can be calculated based on the geometry of the setup. The absolute relationship used for relating Δx (nm) using a PSD, however, needs to include the geometrical factor needed

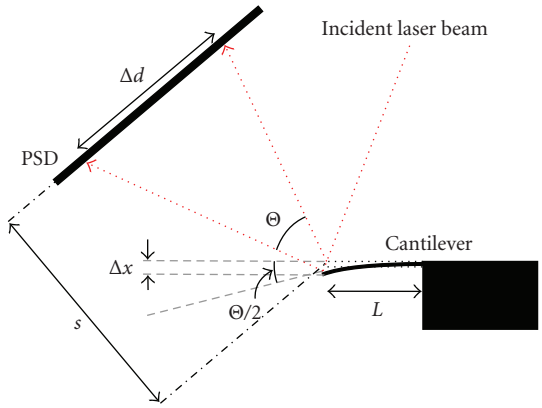

Figure 1: Schematic representation of the geometry of the laser deflection setup. The bending of the cantilever represented by Δx is measured by the PSD as Δd. The active length of the PSD is l_{psd}.

for a particular setup which when incorporated gives the relationship as below:

$$\Delta x = G\frac{I_1 - I_2}{I_1 + I_2}\frac{l_{\text{psd}}}{2}, \tag{2}$$

where $I_1 - I_2$ is the difference signal, and $I_1 + I_2$ is the sum signal obtained from the PSD, and l_{psd} is the active PSD length in mm. It is important to note that Δd (nm) for a PSD is generally defined as (when l_{psd} is defined in mm)

$$\Delta d = \frac{I_1 - I_2}{I_1 + I_2}\frac{l_{\text{psd}}}{2}10^6. \tag{3}$$

Equation (1) gives purely a geometrically calculated value with the aforesaid assumption that if the deflection angle of the laser is Θ, the cantilever bending angle is $\Theta/2$; it includes errors arising from differences in design and actual geometry such as the position and angle of the laser, the angle of the cantilever holder and the reflecting mirror, and the placement of the PSD. A more rigorous approach is needed to take into account not just the theoretical factors but also practical constraints of the setup.

The equipartition theorem relates the thermal energy of a system to its temperature in classical thermodynamics. Thermal noise of a cantilever can be quantified using this theorem [23, 24]. The equipartition theorem states that if a system is in thermal equilibrium, every independent quadratic term in its total energy has a mean value equal to $1/2k_BT$, where k_B is the Boltzmann constant and T is the absolute temperature. The equipartition theorem relates this total energy to the potential energy of a rectangular cantilever with a mean square deflection of the cantilever caused by thermal vibrations as follows [25]:

$$\begin{aligned} \frac{1}{2}\kappa\langle x^2\rangle &= \frac{1}{2}k_BT, \\ \therefore \langle x^2\rangle &= k_BT/\kappa, \end{aligned} \tag{4}$$

where κ is the spring constant of a rectangular cantilever with finite thickness and length provided that the bending is small. From (4), one can determine the thermal displacement of a cantilever provided that the spring constant is known. The deflection factor can hence be calculated if this thermal displacement can be related to the deflection obtained on a PSD.

Combining (2) and (4),

$$\left[G\frac{I_1 - I_2}{I_1 + I_2}\frac{l_{\text{psd}}}{2}\right]^2 = \frac{k_BT}{\kappa}. \tag{5}$$

Hence, deflection factor

$$G = \frac{2}{l_{\text{psd}}}\sqrt{\frac{k_BT}{\kappa\left(\dfrac{I_1 - I_2}{I_1 + I_2}\right)^2}}. \tag{6}$$

The term $((I_1 - I_2)/(I_1 + I_2))^2$ in the above equation is obtained from the PSD signals, using a power spectral analysis program (Virtual instrument, Labview, National Instruments) normalized to the sum signal of the PSD and is the area under the first resonance peak of a cantilever beam of known spring constant. The program essentially obtains the power spectrum which is a computation of the single-sided, scaled spectrum of the time domain signal from the PSD into the frequency domain. For a signal $x(t)$, the complex spectrum is obtained by a fast Fourier transform (FFT) defined as (in the frequency domain)

$$X(f) \equiv \int_{-\infty}^{\infty} x(t)e^{-2\pi ft}dt. \tag{7}$$

This gives, furthermore, the definition of the one sided power spectrum (in Sq. Amplitude/Hz) which is defined as

$$\text{Power spectrum}, \phi(f) \equiv \frac{|X(f)|^2}{n^2} \equiv \frac{|X(f)|\,|X(f)|^*}{n^2}, \tag{8}$$

where n is the number of points in the signal, and * denotes the complex conjugate. The integral of the power spectrum (area under the curve) provides the final value according to the Parseval's theorem which states that the area under the energy spectral density curve is equal to the total energy.

It is important to note that only the area under the first resonance peak is considered in further measurements, neglecting the higher modes since their contribution was seen to be minor (modelled as a simple harmonic oscillator with one degree of freedom). The spring constant of the calibration cantilevers hence needs to be measured as well. There are several methods available to perform such calibration to obtain spring constants [26–32] including the most frequently used thermal noise method. We chose the thermal calibration module in the Asylum MFP-3D AFM [33, 34] (Asylum research, USA) which has been shown to measure the values with relatively good accuracy and reproducibility [34]. The method records the change in PSD position as a function of cantilever angular bending when pressed against a hard surface using a closed loop piezo actuator and then converts it into values for cantilever spring constant using a predetermined sensitivity factor called inverse optical lever sensitivity. With the rest of the terms known in the equation, the calibration factor can be calculated.

Table 1: Manufacturer specifications of the cantilevers used for calibration factor measurement.

Specifications	Mikromasch CSC38/AIBS "B"			NTMDT CSCS12 "E"		
	Min	Typical	Max	Min	Typical	Max
Length (l) μm		350			350	
Width (w) μm		35			35	
Thickness, μm	0.7	1.0	1.3	0.9	1.0	1.1
Resonant frequency (kHz)	7	10	14	8	10	12
Force constant (N/m)	0.01	0.03	0.08	0.02	0.03	0.04

Table 2: Spring constants κ of the calibration cantilevers.

Spring constant	Micromasch B cantilevers		NTMDT cantilevers E	
	B1	B2	E1	E3
κ (pN/nm)	69.66	166.74	32.64	53.13

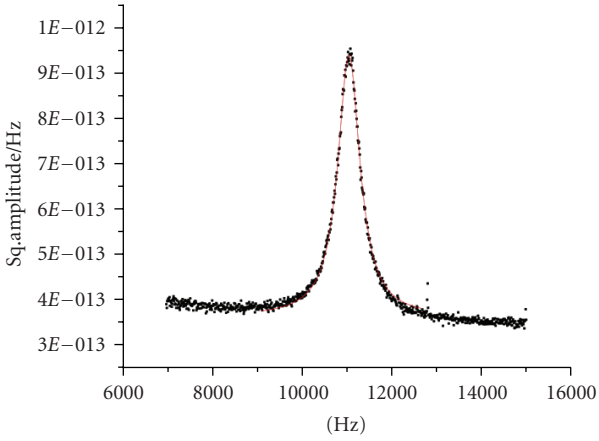

Figure 2: Thermal noise power spectrum of NTMDT cantilever E1 on trial 2 for calibration of Setup 2. The area obtained under the peak after a Lorentzian fit (uniform broadening and best fitting parameters) is later used for determining the calibration factor.

2. Materials and Methods

Different sets of commercially available AFM cantilevers were used namely Mikromasch CSC38/AIBS "B" (Mikromasch, Estonia) and NTMDT CSCS12 "E" (NT-MDT, Russia) cantilevers for the measurement of the thermal noise spectrum and final calibration. The cantilevers were calibrated using the Asylum MFP-3D AFM to get individual values for their spring constants κ. Table 1 enlists manufacturer specifications for these AFM cantilevers.

The power spectrum of the thermal noise was obtained using a 150 kHz band pass position-sensitive detector (SiTek, Sweden). This detector is a modified version of the low-pass 5 Hz sensor which is used for performing static mode biological experiments. A Labview program was used to obtain the averaged power spectrum from the differential and sum signals from the PSD. The parameters for obtaining the power spectrum had to be chosen so as to eliminate effects like aliasing which leads to truncated or artificially small resonance peaks and also electronic noise. Also it was necessary to choose the number of samples and the sampling frequency such that it avoided overloading the system and the data acquisition card (DAQ, National instruments). Keeping in mind all these details and following the Nyquist theorem (signal must be sampled at a rate at least greater than twice the highest frequency component of the signal) the parameters which were chosen for the power spectral analysis were as follows: sampling frequency: 100 kHz, number of samples: 10,000, and number of averages: 5000. The area under the first resonance peak was obtained using a Lorentzian fit in origin graphical software (OriginLab Corporation, USA). The area hence calculated along with the spring constant values was then used to determine the value of G for a particular setup. Two different cantilevers were used for the calibration of each setup with three trials on each cantilever, and the values were finally averaged. Between each trial, the cantilever was taken out of the holder chamber and reinserted. The laser power and the temperature of the chamber were kept constant for all trial measurements.

3. Results

3.1. Geometric Method for Calibration Factor. For our present instrumental scheme, the geometrical calculation for both the setups is the same as derived below. For: $s = 61$ mm (for instrument 1 and 2) and $L = 500\,\mu$m.

Equation (1) can be modified to obtain

$$\Delta x = \frac{\Delta d}{488} \tag{9}$$

Table 3: Calibration factors for the cantilever deflection Setups.

		Area under curve	G	Average G
		Deflection factor G setup 1		
Cant B1 ($\kappa = 69.66$ pN/nm)	Trial 1	$5.20E-10$	2128	2077.5
	Trial 2	$4.51E-10$	2284	
	Trial 3	$4.98E-10$	2175	
Cant B2 ($\kappa = 166.74$ pN/nm)	Trial 1	$2.49E-10$	1986	
	Trial 2	$2.50E-10$	1982	
	Trial 3	$2.70E-10$	1910	
		Deflection factor G setup 2		
Cant E1 ($\kappa = 32.64$ pN/nm)	Trial 1	$7.93E-10$	2517	2679.5
	Trial 2	$5.36E-10$	3062	
	Trial 3	$6.01E-10$	2891	
Cant E3 ($\kappa = 53.13$ pN/nm)	Trial 1	$3.92E-10$	2807	
	Trial 2	$5.50E-10$	2368	
	Trial 3	$5.22E-10$	2432	

Substituting Δd from (3)

$$\Delta x = 2049 \frac{I_1 - I_2}{I_1 + I_2} \frac{l_{\text{psd}}}{2}. \tag{10}$$

Comparing (2) and (10) the deflection factor G from geometric calculations is 2049 for the particular geometry and is the same for any instrument made to this scheme.

3.2. Calibration Factor G Using Equipartition Theorem

3.2.1. Determination of Spring Constants for the Cantilevers Using Asylum AFM. The spring constants for the calibration cantilevers were determined as an average of three trials during which the cantilevers were removed and replaced in the AFM setup in order to average out errors. The averaged values of the cantilevers are summarized in Table 2.

3.2.2. Thermal Noise Data Acquisition from the Instrumental Setups. Calibration factor, G was calculated for two different deflection setups both identical with respect to geometrical design using the previously mentioned cantilever sets. The power spectrum was obtained when keeping the differential signal as close as possible to zero (centre of the PSD) and the sum signal as high as possible. Figure 2 shows a sample powers pectrum obtained for Cantilever E1 on the second trial. According to the power spectrum analysis, we relate the vibrational amplitude in ambient air to the spring constant using (4).

Table 3 summarizes the results for the calibration of the instruments using the above set of cantilevers and substituting the values of the spring constant and the area under the power spectrum into (6).

From the above set of values of the G factor, it can be seen that the two setups differ from the theoretical geometric value and also from each other. The difference between the two values (the value of s differs by ~13.518 mm between the two when back calculated from the obtained calibration factors) indicates that the two setups despite having similar geometry have different travel lengths of the laser from the cantilever surface to the PSD. This could be attributed mainly to the change in position and tilt of the mirror, small differences in the setting up and machining of the home made systems and angles of the cantilever holders and hence the manner in which the lasers spot is reflected by the mirror onto the PSD. It is, hence, important to note that modifications of any kind to such laser deflection systems require a recalibration especially when the differential measurements are close ranged. When compared to results from the geometric method, it is clear that the method we propose shows the variation between individual deflection setups despite their similar geometric design within reasonable error margins (5–10%).

4. Conclusions

The importance of having sensitive measurements especially in systems involving a differential analysis is of foremost significance for ensuring the reliability of cantilever sensor systems. Establishing the occurrence of an event of interest on the cantilever surface using *in situ* reference cantilevers is absolutely essential to eliminate convoluted environmental signals. Hence, a reliable method to calibrate the deflection of the cantilever is mandatory.

We demonstrate here a simple and reliable method for rapid calibration of laser-based deflection systems. Using commercially available AFM cantilevers, we can show that the relationship between the spot movement on the PSD and the actual cantilever deflection can be determined although within the accuracy of the assumptions and the thermal calibration method (~5–10%) [35]. The method was used to calibrate comparable cantilever array systems with a mirror used for deflecting the laser onto the PSD because of space restrictions. This indicates the application of the method

to more complex geometries without the need for accurate measurement of other physical parameters of the geometry.

Acknowledgments

The authors would like to thank the Science Foundation Ireland and F. Hoffman La Roche for their support through research Grants (SFI 00/PI.1/C02, 09IN.1B2623, and Roche 5AAF11).

References

[1] M. Watari, J. Galbraith, H. P. Lang et al., "Investigating the molecular mechanisms of in-plane mechanochemistry on cantilever arrays," *Journal of the American Chemical Society*, vol. 129, no. 3, pp. 601–609, 2007.

[2] F. Huber, M. Hegner, C. Gerber, H. J. Güntherodt, and H. P. Lang, "Label free analysis of transcription factors using microcantilever arrays," *Biosensors & Bioelectronics*, vol. 21, no. 8, pp. 1599–1605, 2006.

[3] J. Mertens, C. Rogero, M. Calleja et al., "Label-free detection of DNA hybridization based on hydration-induced tension in nucleic acid films," *Nature Nanotechnology*, vol. 3, no. 5, pp. 301–307, 2008.

[4] V. Tabard-Cossa, M. Godin, L. Y. Beaulieu, and P. Grütter, "A differential microcantilever-based system for measuring surface stress changes induced by electrochemical reactions," *Sensors and Actuators B*, vol. 107, no. 1, pp. 233–241, 2005.

[5] T. Braun, M. K. Ghatkesar, N. Backmann et al., "Quantitative time-resolved measurement of membrane protein-ligand interactions using microcantilever array sensors," *Nature Nanotechnology*, vol. 4, no. 3, pp. 179–185, 2009.

[6] B. Ilic, Y. Yang, and H. G. Craighead, "Virus detection using nanoelectromechanical devices," *Applied Physics Letters*, vol. 85, no. 13, pp. 2604–2606, 2004.

[7] G. H. Wu, H. Ji, K. Hansen et al., "Origin of nanomechanical cantilever motion generated from biomolecular interactions," *Proceedings of the National Academy of Sciences of the United States of America*, vol. 98, no. 4, pp. 1560–1564, 2001.

[8] J. K. Gimzewski, C. Gerber, E. Meyer, and R. R. Schlittler, "Observation of a chemical reaction using a micromechanical sensor," *Chemical Physics Letters*, vol. 217, no. 5-6, pp. 589–594, 1994.

[9] R. Berger, C. Gerber, J. K. Gimzewski, E. Meyer, and H. J. Güntherodt, "Thermal analysis using a micromechanical calorimeter," *Applied Physics Letters*, vol. 69, no. 1, pp. 40–42, 1996.

[10] T. Braun, N. Backmann, M. Vögtli et al., "Conformational change of bacteriorhodopsin quantitatively monitored by microcantilever sensors," *Biophysical Journal*, vol. 90, no. 8, pp. 2970–2977, 2006.

[11] G. Meyer and N. M. Amer, "Novel optical approach to atomic force microscopy," *Applied Physics Letters*, vol. 53, no. 12, pp. 1045–1047, 1988.

[12] S. Alexander, L. Hellemans, O. Marti et al., "An atomic-resolution atomic-force microscope implemented using an optical lever," *Journal of Applied Physics*, vol. 65, no. 1, pp. 164–167, 1989.

[13] K. A. Walther, J. Brujić, H. Li, and J. M. Fernández, "Sub-angstrom conformational changes of a single molecule captured by AFM variance analysis," *Biophysical Journal*, vol. 90, no. 10, pp. 3806–3812, 2006.

[14] C. A. J. Putman, B. G. De Grooth, N. F. Van Hulst, and J. Greve, "A theoretical comparison between interferometric and optical beam deflection technique for the measurement of cantilever displacement in AFM," *Ultramicroscopy*, vol. 42–44, pp. 1509–1513, 1992.

[15] E. J. Lee, Y. Park, C. S. Kim, and T. Kouh, "Detection sensitivity of the optical beam deflection method characterized with the optical spot size on the detector," *Current Applied Physics*, vol. 10, no. 3, pp. 834–837, 2010.

[16] A. Garcia-Valenzuela and J. Villatoro, "Noise in optical measurements of cantilever deflections," *Journal of Applied Physics*, vol. 84, no. 1, pp. 58–63, 1998.

[17] A. Garcia-Valenzuela, "Limits of different detection schemes used in the optical beam deflection method," *Journal of Applied Physics*, vol. 82, no. 3, pp. 985–988, 1997.

[18] Z. Y. Hu, T. Seeley, S. Kossek, and T. Thundat, "Calibration of optical cantilever deflection readers," *Review of Scientific Instruments*, vol. 75, no. 2, pp. 400–404, 2004.

[19] M. Godin, V. Tabard-Cossa, P. Grütter, and P. Williams, "Quantitative surface stress measurements using a microcantilever," *Applied Physics Letters*, vol. 79, no. 4, pp. 551–553, 2001.

[20] T. Miyatani and M. Fujihira, "Calibration of surface stress measurements with atomic force microscopy," *Journal of Applied Physics*, vol. 81, no. 11, pp. 7099–7115, 1997.

[21] N. P. D'Costa and J. H. Hoh, "Calibration of optical lever sensitivity for atomic force microscopy," *Review of Scientific Instruments*, vol. 66, no. 10, pp. 5096–5097, 1995.

[22] L. Y. Beaulieu, M. Godin, O. Laroche, V. Tabard-Cossa, and P. Grütter, "Calibrating laser beam deflection systems for use in atomic force microscopes and cantilever sensors," *Applied Physics Letters*, vol. 88, no. 8, Article ID 083108, 3 pages, 2006.

[23] G. Binnig, "Force microscopy," *Ultramicroscopy*, vol. 42–44, pp. 7–15, 1992.

[24] Y. Martin, C. C. Williams, and H. K. Wickramasinghe, "Atomic force microscope-force mapping and profiling on A sub 100-Å scale," *Journal of Applied Physics*, vol. 61, no. 10, pp. 4723–4729, 1987.

[25] H. J. Butt and M. Jaschke, "Calculation of thermal noise in atomic force microscopy," *Nanotechnology*, vol. 6, no. 1, pp. 1–7, 1995.

[26] R. Levy and M. Maaloum, "Measuring the spring constant of atomic force microscope cantilevers: thermal fluctuations and other methods," *Nanotechnology*, vol. 13, no. 1, pp. 33–37, 2002.

[27] S. K. Jericho and M. H. Jericho, "Device for the determination of spring constants of atomic force microscope cantilevers and micromachined springs," *Review of Scientific Instruments*, vol. 73, no. 6, pp. 2483–2485, 2002.

[28] J. L. Hutter and J. Bechhoefer, "Calibration of atomic-force microscope tips," *Review of Scientific Instruments*, vol. 64, no. 7, pp. 1868–1873, 1993.

[29] J. E. Sader, J. W. M. Chon, and P. Mulvaney, "Calibration of rectangular atomic force microscope cantilevers," *Review of Scientific Instruments*, vol. 70, no. 10, pp. 3967–3969, 1999.

[30] H. L. Ma, J. Jimenez, and R. Rajagopalan, "Brownian fluctuation spectroscopy using atomic force microscopes," *Langmuir*, vol. 16, no. 5, pp. 2254–2261, 2000.

[31] J. P. Cleveland, S. Manne, D. Bocek, and P. K. Hansma, "A nondestructive method for determining the spring constant of cantilevers for scanning force microscopy," *Review of Scientific Instruments*, vol. 64, no. 2, pp. 403–405, 1993.

[32] J. E. Sader, I. Larson, P. Mulvaney, and L. R. White, "Method for the calibration of atomic force microscope cantilevers,"

Review of Scientific Instruments, vol. 66, no. 7, pp. 3789–3798, 1995.

[33] D. A. Walters, J. P. Cleveland, N. H. Thomson et al., "Short cantilevers for atomic force microscopy," *Review of Scientific Instruments*, vol. 67, no. 10, pp. 3583–3590, 1996.

[34] R. Proksch, T. E. Schäffer, J. P. Cleveland, R. C. Callahan, and M. B. Viani, "Finite optical spot size and position corrections in thermal spring constant calibration," *Nanotechnology*, vol. 15, no. 9, pp. 1344–1350, 2004.

[35] N. A. Burnham, X. Chen, C. S. Hodges et al., "Comparison of calibration methods for atomic-force microscopy cantilevers," *Nanotechnology*, vol. 14, no. 1, pp. 1–6, 2003.